Published in final edited form as:

J Allergy Clin Immunol. 2018 October ; 142(4): 1297–1310.e11. doi:10.1016/j.jaci.2017.10.031.

ORAI1 mutations abolishing store-operated Ca^{2+} entry cause anhidrotic ectodermal dysplasia with immunodeficiency (EDA-ID)

Jayson Lian, B.A.[1,†], **Mario Cuk, M.D., Ph.D.**[2,†], **Sascha Kahlfuss, M.D.**[1,†], **Lina Kozhaya, Ph.D.**[3], **Martin Vaeth, Ph.D.**[1], **Frédéric Rieux-Laucat, Ph.D.**[4,5], **Capucine Picard, M.D., Ph.D.**[5,6], **Melina J. Benson, B.A.**[1], **Antonia Jakovcevic, M.D.**[7], **Karmen Bilic, M.D.**[8], **Iva Martinac, M.D.**[2], **Peter Stathopulos, Ph.D.**[9], **Imre Kacskovics, M.D.**[10], **Thomas Vraetz, M.D.**[11], **Carsten Speckmann, M.D.**[11,12], **Stephan Ehl, M.D.**[11,12], **Thomas Issekutz, M.D.**[13], **Derya Unutmaz, M.D.**[3], and **Stefan Feske, M.D.**[1]

[1]Department of Pathology, New York University School of Medicine, New York, NY, USA

[2]Department of Pediatrics, University Hospital Centre Zagreb, University of Zagreb, School of Medicine, Zagreb, Croatia

[3]The Jackson Laboratory for Genomic Medicine, Farmington, CT, USA

[4]INSERM UMR 1163, Laboratory of The Immunogenetics of Pediatric Autoimmune Diseases, Paris, France

[5]INSERM UMR1163, Imagine Institute, Paris Descartes-Sorbonne Paris Cité University, Paris, France

[6]Study Center for Primary Immunodeficiencies, Necker-Enfants Malades Hospital, Assistance Publique Hôpitaux de Paris (APHP), Necker Medical School, Paris, France

[7]Department of Pathology and Cytology, University Hospital Centre Zagreb, Zagreb, Croatia

[8]Clinical Institute of Laboratory Diagnosis, University Hospital Centre Zagreb, Zagreb, Croatia

[9]Department of Physiology and Pharmacology, Schulich School of Medicine and Dentistry, Western University, London, Ontario, Canada

[10]ImmunoGenes, Budapest 2092, Hungary

[11]Department of Pediatric Hematology and Oncology, Center for Pediatrics, Medical Center, University of Freiburg, Faculty of Medicine, University of Freiburg, Freiburg, Germany

[12]Center for Chronic Immunodeficiency, Medical Center, University of Freiburg, Faculty of Medicine, Freiburg, Germany

Corresponding author: Stefan Feske, Department of Pathology, New York University School of Medicine, New York, NY 10016, USA; Telephone: +1-212-263-9066; feskes01@nyumc.org.

[†]These authors contributed equally

Conflict of interest: S.F. is a cofounder of Calcimedica; the other authors declare no conflict of interest.

[13]Division of Immunology, Department of Pediatrics Dalhousie University, Halifax B3K 6R8, Canada

Abstract

Background—Store-operated Ca^{2+} entry (SOCE) through Ca^{2+} release-activated Ca^{2+} (CRAC) channels is an essential signaling pathway in many cell types. CRAC channels are formed by ORAI1, ORAI2 and ORAI3 proteins and activated by stromal interaction molecule 1 (STIM1) and STIM2. Mutations in *ORAI1* and *STIM1* genes that abolish SOCE cause a combined immunodeficiency (CID) syndrome that is accompanied by autoimmunity and non-immunological symptoms.

Objective—Molecular and immunological analysis of patients with CID, anhidrosis and ectodermal dysplasia of unknown etiology.

Methods—DNA sequencing of *ORAI1* gene, modeling of mutations on ORAI1 crystal structure, analysis of ORAI1 mRNA and protein expression, measurements of SOCE, immunological analysis of peripheral blood lymphocyte populations by flow cytometry, histological and ultrastructural analysis of patient tissues.

Results—We identified 3 novel autosomal recessive mutations in *ORAI1* in unrelated kindreds with CID, autoimmunity, ectodermal dysplasia with anhidrosis (EDA) and muscular dysplasia. The patients were homozygous for p.V181SfsX8, p.L194P and p.G98R mutations in the *ORAI1* gene that suppressed ORAI1 protein expression and SOCE in the patients' lymphocytes and fibroblasts. Besides impaired T cell cytokine production, ORAI1 mutations were associated with strongly reduced numbers of invariant natural killer (iNKT) and regulatory T (Treg) cells, and altered composition of γδ T cell and NK cell subsets.

Conclusion—*ORAI1* null mutations are associated with reduced numbers of iNKT and Treg cells that likely contribute to the patients' immunodeficiency and autoimmunity. ORAI1 deficient patients suffer from dental enamel defects and anhidrosis representing a new form of anhidrotic ectodermal dysplasia with immunodeficiency (EDA-ID) that is distinct from previously reported patients with EDA-ID due to mutations in the NF-kB signaling pathway (*IKBKG* and *NFKBIA*).

Keywords

CRAC channel; Store-operated Ca^{2+} entry (SOCE); calcium; ORAI1; T cells; Treg cells; iNKT cells; immunodeficiency; CID; anhidrotic ectodermal dysplasia (EDA)

Introduction

Ca^{2+} is an important second messenger required for the activation of lymphocytes and other cell types within and outside the immune system. Ca^{2+} influx in lymphocytes is initiated by antigen receptor binding that results in the activation of phospholipase Cγ(PLC-γ) and production of inositol-1,4,5-trisphosphate (IP_3), which binds to IP_3 receptors (IP_3R) in the endoplasmic reticulum (ER) membrane. The opening of IP_3Rs mediates the release of Ca^{2+} from the ER and activation of stromal interaction molecule (STIM) 1 and STIM2 that are located in the ER membrane [1, 2]. Activated STIM1 and STIM2 bind to ORAI1, a tetraspanning plasma membrane protein that forms the pore of the CRAC channel [3–5].

Opening of the CRAC channel results in Ca^{2+} influx, or store-operated Ca^{2+} entry (SOCE) because it is regulated by the filling state of ER Ca^{2+} stores. SOCE is an essential Ca^{2+} signaling pathway in lymphocytes and required for the activation of many Ca^{2+}-dependent enzymes and transcription factors that control the differentiation, proliferation and function of cells in the immune system [6].

The importance of SOCE for immunity is apparent from autosomal recessive (AR) null mutations in *ORAI1* and *STIM1* genes that cause a combined immunodeficiency (CID) syndrome characterized by recurrent and severe viral, bacterial and fungal infections [3, 7–11]. In contrast to Severe Combined Immunodeficiency (SCID) patients that lack T cells and/or B cells [12], the numbers of T and B cells are largely normal in STIM1- and ORAI1-deficient patients [13]. However, the function of T cells, natural killer (NK) cells and potentially other immune cells is impaired. In addition, patients present with lymphoproliferation (lymphadenopathy, hepatosplenomegaly) and autoimmunity that is characterized by hemolytic anemia and/or thrombocytopenia associated with auto-antibodies against red blood cells and platelet glycoproteins [10]. Besides immune dysregulation, patients lacking SOCE suffer from congenital muscular hypotonia, defects in dental enamel development and anhidrosis [13]. It is noteworthy that the clinical phenotype of patients with AR *ORAI1* and *STIM1* mutations is very similar (although *ORAI1* mutations may cause a more severe immunodeficiency requiring hematopoietic stem cell transplantation, HSCT, within the first year of life). Because of the conserved clinical phenotype resulting from *ORAI1* and *STIM1* mutations, we have named the resulting disease syndrome CRAC channelopathy [14]. *ORAI1* and *STIM1* mutations are rare and limited patient material is available to study the effects of impaired CRAC channel function on immune cell populations and function [9]. The full clinical spectrum and immune dysfunction associated with CRAC channel dysfunction therefore remains to be carefully studied. The identification and characterization of CRAC channel mutations is essential to understand the molecular regulation of CRAC channels and their role in human immunity and the physiological function of other organs.

We here identify 4 patients from unrelated kindreds with 3 novel autosomal recessive mutations in *ORAI1.* All mutations resulted in abolished ORAI1 protein expression and SOCE. *ORAI1* mutations were associated with impaired T cell function and reduced numbers of iNKT and Treg cells whereas γδ T cells and NK cell subsets were altered in their composition. Reduced lymphocyte function and composition likely contribute to the patients' CID whereas decreased Treg cell numbers may account for their lymphoproliferation and autoimmunity. All 4 patients suffered from amelogenesis imperfecta and anhidrosis. Null mutations in *ORAI1* represent a new form of EDA-ID that is distinct from EDA-ID observed in patients with mutations in genes (*IKBKG*, *NFKBIA*) mediating NF-κB signaling [15, 16].

Methods

Patients

Case reports for patients P1–P4 and P6 are provided in the Online Repository and summarized in Table 1.

Cell culture

Patient and healthy donor (HD) fibroblasts were cultured in RPMI 1640 medium supplemented with 10% FCS, 1% L-glutamine, 1% HEPES, and 1% Penicillin/Streptomycin (all from Mediatech, Manassas, VA). SOCE-deficient PBMC from P3 and P6 before their first and second HSCT, respectively, and a HD were isolated from whole blood by Ficoll density centrifugation (GE Healthcare, Marlborough, MA) and stimulated with irradiated buffy coat cells, irradiated B cells, PHA (1 μg/ml) and recombinant human IL-2 (50 U/ml) for 10–12 days.

Flow cytometry

For immune phenotyping of patient blood, 5×10^5 fresh or frozen PBMCs from patients and healthy donors (HDs) were incubated with antibodies against cell surface proteins and the fixable Viability Dye eFluor506 (eBioscience, Carlsbad, CA) followed by antibody staining of intracellular molecules using the IC staining kit (eBioscience, Carlsbad, CA). A complete list of antibodies and conjugated fluorochromes can be found in Table E3. Samples were acquired on a LSRII flow cytometer (BD Biosciences) and analyzed using the FlowJo software (Tree Star). The gating strategy for the identification of NK, iNKT and γδ T cells is shown in Fig. E4. For ORAI1 cell surface protein expression, patient and HD control fibroblasts were stained with an Alexa Fluor 647-conjugated anti-human ORAI1 monoclonal antibody (2C1.1) that recognizes an epitope in the second extracellular loop (ECL2) of ORAI1 (kind gift of H. McBride, Amgen). Unstained cells served as negative control.

Time-lapse Ca^{2+} imaging

Ca^{2+} imaging was performed as described [17]. Briefly, cells were loaded with Fura-2 AM (Invitrogen) and stimulated as indicated in figures. Fura-2 emission ratios (F340/380) were calculated every 5s. 20–100 cells per experiments were analyzed.

Additional methods and case reports are available in the online repository accompanying this article.

Results

Identification of patients with novel mutations in *ORAI1*

We investigated the gene defects in 4 patients from 3 independent kindreds who presented with a combination of severe infections in the first year of life, muscular hypotonia, tooth defects and anhidrosis. Patient 1 (P1, A-II-1, Fig. 1A) was born to consanguineous parents. Early after birth, he suffered from viral infections and at six months he developed a severe *Pneumocystis jiroveci* pneumonia (for details see case report in Methods in the Online Repository and Table 1). In addition to immunodeficiency, P1 presented with congenital muscular hypotonia and symptoms of EDA (see below). Because his symptoms were consistent with CRAC channelopathy due to mutations in either *ORAI1* or *STIM1* genes [9, 10, 13, 18], we performed genomic DNA sequencing of both genes. P1 was homozygous for a single cytosine nucleotide deletion at position 541 of the *ORAI1* mRNA (c.del541C). Both parents were heterozygous for the same mutation (Fig. 1A and **E1A)**. The *ORAI1* del541C

mutation results in a frameshift and subsequent premature stop codon (V181SfsX8) in the third transmembrane domain (TM3) of ORAI1 protein (Fig. 1B).

Patient 2 (P2, B-II-1, Fig. 1C) was born to nonrelated parents. She presented acutely at 2 months of age with meningitis, pneumonia and gastroenteritis characterized by opisthotonus, tachycardia, tachypnea, hyperpyrexia, vomiting, diarrhea and dehydration. At 3.5 months, P2 deteriorated due to sepsis, massive bilateral *Staphylococcus aureus* pneumonia and Cytomegalovirus (CMV) pneumonitis. P2 continued to suffer from multiple life-threatening infections with viral, bacterial and fungal pathogens to which she succumbed at 7.5 months (see case report in Methods in the Online Repository and Table 1). Genomic DNA sequencing revealed that she was homozygous for an AR missense mutation (c.T581C) in *ORAI1*. Both parents of P2 and her sister were heterozygous for the same mutation (Fig. 1C and **E1B)**. The n.T581C mutation causes substitution of a single amino acid (p.L194P) in TM3 of ORAI1 protein (Fig. 1D).

Patient 3 (P3, C-II-2, Fig. 1E) was born to nonrelated parents (Fig. 1E) and soon after birth developed an acute bronchiolitis caused by Respiratory Syncitial Virus (RSV). In the first months of his life, he suffered from various recurrent viral and bacterial infections including persistent CMV infection (see case report in Methods in the Online Repository and Table 1). Genomic DNA sequencing revealed that P3 is homozygous for a missense mutation (c.G292C) in *ORAI1*. The mutation results in the substitution of a single amino acid (p.G98R) within TM1 of ORAI1 protein (Fig. 1F). Both parents of P3 and a healthy brother were heterozygous for the same mutation, whereas his older sister P4 (C-II-1) was homozygous for the same *ORAI1* p.G98R mutation (Fig. 1E and Fig. E1C). From ~3.5 months of age, she suffered from frequent, severe and prolonged respiratory tract infections caused by various bacterial, fungal and viral pathogens including CMV (see case report in Methods in Online Repository and Table 1). In her second year of life, P4 developed respiratory failure requiring mechanical ventilation. She continued to suffer from multiple infections including CMV that caused pneumonitis, chorioretinitis with blindness, colitis and encephalitis, from which she died at the age of 2.5 years. In addition, P4 suffered from multiple episodes of autoimmune hemolytic anemia (AIHA) and thrombocytopenia (ITP) associated with gastrointestinal bleeding.

Modelling of *ORAI1* mutations on the crystal structure of dOrai

The scaled Combined Annotation-Dependent Depletion (CADD) scores of the three *ORAI1* mutations were 35.0 (P1), 26.5 (P2) and 32.0 (P3, P4), indicating that they are within the top 1% (P2) and 0.1% (P1, P3, P4) of the most deleterious variants in the human genome. To understand the effects of the mutations on ORAI1 function, we generated a homology model of the human ORAI1 protein structure that is based on the *Drosophila melanogaster* Orai (dOrai) crystal structure [19]. Like dOrai, ORAI1 is a tetraspanning plasmamembrane protein that assembles into a functional hexameric CRAC channel complex [3, 19, 20]. The channel pore is formed my an inner ring of six TM1 domains that is surrounded by concentric rings of TM2/TM3 and TM4 domains. We previously described mutations in TM1 and TM3 that either abolish protein expression or result in non-functional proteins [3, 9]. Fig. 1G shows the position of the three residues mutated in patients P1–P4 in the human ORAI1 protein

structure model. G98 is located in TM1 and faces the lumen of the open CRAC channel pore (Fig. 1G, H) [21]. The large and positively charged side chain of the arginine (R) substitution at G98 is predicted to occlude the CRAC channel pore (Fig. 1H). L194 is located towards the extracellular end of the TM3 α-helix (Fig. 1G, I). This position is in the same lateral plane as the pore lining E106 residue in TM1 that is involved in Ca^{2+} binding [19, 22] and in close proximity (<5 Å) to several hydrophobic residues of TM1 that surround E106 residue (Fig. 1I). We hypothesized that the location of the G98R and L194P mutations in TM1 and TM3, respectively, likely interferes with ORAI1 protein function or stability.

ORAI1 mutations abolish SOCE and protein expression

To investigate whether *ORAI1* mutations impair CRAC channel function, we measured Ca^{2+} influx in fibroblasts of the 3 patients and HDs. Stimulation of cells with thapsigargin in the absence of extracellular Ca^{2+} resulted in a transient rise in the intracellular Ca^{2+} concentration ($[Ca^{2+}]_i$) due to Ca^{2+} release from ER stores, which was comparable in patient and HD cells (Fig. 2A–C). Re-addition of extracellular Ca^{2+} resulted in strong SOCE in HD fibroblasts, whereas SOCE was strongly reduced or absent in fibroblasts of all three patients (Fig. 2A–C and G–I). To validate that abolished SOCE in patient fibroblasts was caused by the mutations in *ORAI1*, we retrovirally transduced fibroblasts with wildtype ORAI1 or STIM1 (as control). We found that Ca^{2+} influx in fibroblasts from all three patients was restored by ectopic expression of ORAI1 whereas STIM1 had no effect (Fig. 2D–F and G–I). Collectively, these data demonstrate that the mutations in *ORAI1* are responsible for abolished SOCE in P1, P2 and P3.

To experimentally test the effects of the mutations on channel expression, we measured *ORAI1* mRNA and protein levels in the patients' cells. *ORAI1* mRNA was not significantly reduced in P1–P3 compared to healthy donor (HD) controls (Fig. 3A–C). To analyze ORAI1 protein expression, we incubated fibroblasts of P1–P3 and HDs with a monoclonal antibody that recognizes an extracellular domain of human ORAI1 [23]. Whereas ORAI1 was detectable at the surface of HD fibroblasts, no ORAI1 expression was found in fibroblasts of the 3 patients (Fig. 3D–F). Given normal mRNA expression, the V181SfsX8, L194P and G98R mutations likely abolish ORAI1 expression by interfering with protein stability.

ORAI1 mutations impair T cell function and perturb iNKT, NK, Treg and γδ T cell populations

Patients with mutations in *ORAI1* suffer from CID with life-threatening infections. The early onset, severity and type of infections in ORAI1-deficient patients resembles that observed in patients with SCID. Unlike SCID, however, the development of conventional T and B cells is largely preserved in the limited number of patients with *ORAI1* null mutations reported to date [13]. We here confirm that patients P1–P4 have numbers of conventional $CD3^+$ T and $CD19^+$ B cells that are normal or only slightly outside the normal range (Table 1 and Table E1). Some ORAI1-deficient patients (P3, P4) had an increased CD4:CD8 T cell ratio that was not present in P1 and P2 or previously published patients and may be due to their chronic systemic infections (Table E1).

To better understand the role of CRAC channels in lymphocyte development and function, we analyzed T cells from P3 and a previously reported patient (P6) with a null mutation in *ORAI1* (p.R91W) that abolishes SOCE [3] because PBMC from other patients (P1, P2, P4) were not available for an in-depth analysis. We first confirmed that T cells isolated from P3 before HSCT have a similar defect in SOCE as his fibroblasts (Fig. 4A). Functionally, the T cells of P1 and P3 showed strongly reduced or absent proliferation in response to PHA, other mitogens and specific antigens (Table E1). In addition, stimulation of ORAI1-deficient T cells resulted in strongly decreased production of IFN-γ(P2, P4) and IL-4 (P4) (Table 1). Impaired production of IL-2, TNFα and IL-22 was also observed in $CD45RO^+$ effector T cells of P6 isolated as 20 years of age (Fig. 4B). (Note that P6 was treated with HSCT at 4 months, but had completely lost donor chimerism in his lymphocytes, and thus SOCE, by 19 years of age [24–26]). These defects are consistent with previous reports of other ORAI1 and STIM1-deficient patients demonstrating a critical role of SOCE in cytokine production and proliferation of T cells [8, 9, 27, 28].

To evaluate the effects of ORAI1 deficiency on lymphocyte development, we analyzed PBMC of P3 and P6. The analysis of $CD4^+$ and $CD8^+$ T cells of P6 showed reduced numbers of naïve $CD45RO^-$ $CCR7^+$ T cells in both subsets compared to a HD control (Fig. 4C). We observed a reciprocal increase of $CD4^+$ $CD45RO^+$ $CCR7^+$ central and $CD8^+$ $CD45RO^+$ $CCR7^-$ effector memory T cells in P6 compared to a healthy donor (HD) control (Fig. 4C, middle and lower panels). The loss of naive $CD45RA^+$ T cells and concomitant expansion of $CD45RO^+$ or $HLA\text{-}DR^+$ activated T cells is also found in P1 and P3 (Table 1 and Table E1) as well as previously reported SOCE-deficient patients [8, 9, 27].

ORAI1-deficient patients P2, P3 and P4 suffered from AIHA, autoimmune thrombocytopenia, neutropenia and antiphospholipid syndrome (case reports and Table 1), suggesting that SOCE is required for maintaining immunological tolerance. We therefore tested if lack of ORAI1 in patients affects their numbers of Treg cells. P6 showed a profound reduction of $CD27^+$ $FOXP3^+$, $CD45RO^-$ $FOXP3^+$ and $CD45RO^+$ $FOXP3^+$ Tregs compared to a HD control (Fig. 4D) [28]. Similarly, P3 showed strongly decreased percentages of $CD25^+$ $FOXP3^+$ Treg cells and $CD25^+$ $CD127^{low}$ T cells (Fig. 4E), which express high levels of FOXP3 and effectively suppress T cell proliferation [29]. The strong reduction of Treg cells in P3 was observed in $CD45RA^+$ $FOXP3^{low}$ naive and $CD45RA^-$ $FOXP3^+$ activated Treg cells (Fig. 4E). The decrease in Treg cells likely contributes to the loss of naive T cells, autoimmunity and lymphadenopathy observed in P3 and other ORAI1-deficient patients.

Deletion of *Stim1* and *Stim2* in murine T cells was shown to impair the development of agonist-selected T cells including, besides Treg cells, iNKT cells and $TCR\alpha\beta^+$ $CD8\alpha\alpha^+$ intestinal intraepithelial lymphocytes [30]. We therefore analyzed iNKT cells together with NK cells in PBMCs from the 20-year-old P6 compared to 23 unrelated adult HD controls. Within the NK cell compartment, the numbers of $CD56^+$ $CD16^+$ NK cells, the main population in human blood, were reduced whereas $CD56^-$ $CD16^+$ NK cells were increased compared to HD controls (Fig. 5A, D). More strikingly, we observed a complete absence of $CD3^+$ TCR $V\alpha24^+J\alpha18^+$ iNKT cells in P6 compared to HD controls (Fig. 5B, D). Similar defects were observed analyzing PBMC of the 5-month-old P6 (not shown). Given the important role of iNKT cells in immunity to bacterial and viral infections, the lack of iNKT

cells likely contributes to the patient's CID [31]. Another non-conventional T cell population that combines features of adaptive and innate immune cell types are γδ T cells [32]. We observed markedly increased frequencies of $CD8^+$ γδ as well as $CD4^-CD8^-$ γδ T cells in PBMC of the 20-year-old P6 compared to HD controls (Fig. 5C, D), which may be a response to the patient's chronic infections. Collectively, our findings indicate that SOCE is required for the development of agonist-selected iNKT and Tregs, whose marked reduction in ORAI1 deficient patients likely contributes to their CID and autoimmunity.

ORAI1 null mutations cause EDA

Besides CID and autoimmunity, *ORAI1* mutations were associated with congenital, non-progressive muscular hypotonia affecting the facial, axial and respiratory musculature and causing partial iris hypoplasia (Fig. E2A, B). Whereas muscle biopsies of P2 and P3 did not reveal abnormalities in H&E staining (Fig. E2C and not shown), ATPase staining of a muscle biopsy of P1 showed a predominance of type 1 and paucity of type 2 muscle fibers (Fig. E2D). At the ultrastructural level, muscle biopsies of P2 and P3 revealed defects in mitochondrial morphology and viability (Fig. E2E–K) suggesting, together with impaired electron transport chain function (see case reports in Methods in Online Repository), that ORAI1 deficiency may cause muscular hypotonia through mitochondrial dysfunction. This interpretation is consistent with impaired mitochondrial function in fibroblasts of ORAI1 and STIM1-deficient patients [33] and T cells of *Stim1/Stim2*-deficient mice (Vaeth et al., paper in press). By contrast, gain-of-function mutations in *ORAI1* and *STIM1* are characterized by tubular aggregate myopathy (TAM) [13, 34, 35], indicating that precise homeostasis of SOCE is required to maintain skeletal muscle integrity and function.

Null mutations in *ORAI1* were furthermore associated with EDA (Fig. E3 and Table E2). P1–P4 were unable to sweat and lacked sweat production tested by pilocarpin iontophoresis (Table 1 and **E2**). P3 and P4 had dry and exfoliate skin, and at 3 and 6 months of age, respectively, they showed signs of heat intolerance and thermoregulatory instability characterized by several attacks of facial flashing accompanied by tachycardia, tachypnea and hypertension. A skin biopsy of P1 showed the presence of eccrine sweat glands in the dermis, demonstrating that anhidrosis is not due to a defect in sweat gland development. In addition, ORAI1-deficient patients had severe enamel defects diagnosed as hypocalcified amelogenesis imperfecta (type III) (Table E3). The teeth of P1 at 8 months showed pitted enamel hypoplasia and hypomineralization of incisors. He developed multiple dental abscesses and six of his permanent teeth have been extracted and virtually all other teeth had to be capped. The teeth of P3 showed severely cracked, chipped and absent enamel with exposure of the underlying dentine (yellow) and excessive wear (Fig. E3C). The teeth of his sister P4 at 10 months of age showed yellowish discoloration (Table 1). Similar defects in enamel formation were reported in other patients with null mutations in *ORAI1* and *STIM1* [13] (Table E2). Another feature of EDA in P1–P4 was their sparse, thin and brittle hair (Fig. E3D, Table 1 and **E2**). Taken together, mutations in *ORAI1* (and *STIM1*) that abolish SOCE represent a new form of EDA and ID, which is distinct from EDA-ID due to mutations in the NF-kB signaling pathway [16, 36, 37].

Discussion

We here describe 3 novel mutations in *ORAI1* that abolish SOCE and cause CID, autoimmunity and EDA in infant patients. One of the mutations (ORAI1 p.V181SfsX8) truncates the ORAI1 protein at the beginning of TM3, preventing expression of a functional protein in the plasma membrane. The other 2 mutations (ORAI1 p.G98R and L194P) abolish ORAI1 protein expression most likely by interfering with protein stability. Modelling the mutations on the crystal structure model of human ORAI1 indicates that substitution of G98 in TM1 by arginine (G98R) occludes the CRAC channel pore or results in sterical clashes of the large and positively charged arginine side chains when the mutant ORAI1 p.G98R proteins are assembled into the hexamer channel, thus destabilizing the ORAI1 protein complex. G98 is critical for ORAI1 function. It was suggested to function as a gating hinge that controls the opening of the ORAI1 channel [38]. Other studies showed that G98 lines the pore when the ORAI1 channel is activated by STIM1 [39, 40] but is replaced by neighboring F99 through a rotational movement of the TM1 α-helix when the channel is closed [19, 21]. The importance of G98 for CRAC channel function is emphasized by engineered mutations that either abolish (G98A) or constitutively activate (G98D, G98P) CRAC channel function [38]. In humans, heterozygosity for a ORAI1 p.G98S mutation causes constitutive Ca^{2+} influx and TAM [34]. By contrast, the G98R mutation we identified here abolishes SOCE by preventing ORAI1 protein expression. L194 is located in TM3 which does not line the pore but forms a concentric ring of α-helices surrounding the inner ring of TM1 domains. However, L194 is located at the extracellular end of TM3 and maps closely (<5 Å) to several hydrophobic residues in TM1 next to E106 that is the Ca^{2+} binding site in the selectivity filter of the CRAC channel [19, 22]. The human ORAI1 protein structure model predicts that breaking of the TM3 helix by proline substitution of L194 disrupts the TM3 backbone hydrogen bonding and perturbs the extensive network of hydrophobic interactions centered around L194. The L194P mutation thus likely interferes with the stability of individual ORAI1 proteins, preventing the proper assembly of ORAI1 subunits into a hexameric channel structure and enhancing the degradation of ORAI1 proteins.

Null mutations in *ORAI1* result in CID and increased susceptibility to a variety of viral, bacterial and fungal pathogens as apparent from the broad spectrum of infections observed in P1–P4. One cause of infections is impaired T cell function, which is characterized by defective proliferation after mitogen or antigen stimulation and markedly reduced production of cytokines including IL-2, IL-22, TNFα and IFNγ. These defects are consistent with similar findings in other patients with *ORAI1* and *STIM1* mutations [8–10, 28]. ORAI1-deficient T cells, however, are not completely unresponsive, as demonstrated by the expansion of $CD45RO^+$ memory $CD4^+$ and $CD8^+$ T cells, which may be due to the known role of ORAI1, STIM1 and SOCE in promoting T cell apoptosis [25, 41].

In addition to impaired T cell function, we here report marked perturbations in several lymphocyte populations including iNKT, NK, Treg and γδ T cells in ORAI1 deficient patients that likely contribute to their CID and autoimmunity. In particular, the lack of TCR $Vα24^+Jα18^+$ iNKT cells may impair immunity to bacterial and viral infections given the important role of iNKT cells in recognizing bacterial lipid and glycolipid antigens [31]. Reduced iNKT cells were also found in a patient lacking *STIM1* expression [8] and in *Stim1/*

Stim2-deficient mice [30], suggesting that SOCE is critical for the development of this agonist-selected lymphocyte population. Total NK cell numbers were in the low normal range in P1–P4. In P6, for whom PBMCs were available for in-depth analysis, the frequencies of $CD56^+$ $CD16^+$ NK cells was reduced whereas $CD56^-$ $CD16^+$ NK cells were increased. The increase in $CD56^-$ $CD16^+$ NK cells is reminiscent of the expansion of a similar, highly dysfunctional population of NK cells in chronically HIV or HCV-infected individuals [42, 43]. To which degree the altered NK cell subsets contributes to CID in ORAI1-deficient patients remains to be tested. In contrast to iNKT and of $CD56^+$ $CD16^+$ NK cells, the numbers of $CD8^+$ and $CD4^-CD8^-$ γδ T cells were increased in P6. The majority of these γδ T cells were $CD3^{low}$ $γδTCR^{high}$, which are thought to mostly belong to the Vδ1 subset [44] and may be derived from intestinal tissues [45]. Vδ1 T cells can be expanded by inflammatory cytokines induced by microbial components [46]. Thus, it is conceivable that dysbiosis or microbial translocation due to disruption of the immune system in the gut results in the expansion of these γδ T cells in the patient. Alternatively, expansion of γδ T cells also occurs in CMV infection [47], which is common in ORAI1 deficient patients. In this context it is noteworthy that increased γδ T cells were observed in the 20-year-old patient P6 who suffered from CMV infection, but not in the 5-months-old P6, in whom $CD8^+$ γδ T cells were normal and $CD4^-CD8^-$ γδ T cells were decreased. It is therefore likely that the increased $CD4^-CD8^-$ γδ T cells in the 20-year-old patient are secondary to his CMV infection and/or his reduced numbers of Treg cells.

Besides CID, ORAI1-deficient patients reported here suffered from AIHA (P2–P4), ITP (P2, P4) and autoimmune neutropenia (P4). Autoantibodies (ANA, ANCA, anti-cardiolipin, anti-β2 glycoprotein) were detected in P3 and P4. We here show that null mutations in *ORAI1* are associated with reduced numbers of $Foxp3^+$ Tregs (P3, P6). This finding is consistent with similar observations in patients with null mutations in *STIM1* [8, 10] and mice lacking *Orai1/Orai2* [48] or *Stim1/Stim2* [28, 30, 49]. Besides decreased thymic-derived Treg cells, mice lacking *Stim1/Stim2* also had a defect in the differentiation of inducible (peripheral) Treg cells [25] and follicular Treg (T_{FR}) cells [28]. The latter defect results in autoantibody production including ANA and anti-dsDNA antibodies, which is associated with spontaneous GC formation and an increase in GC B cells [28]. Because *Stim1/Stim2*-deficient mice also have reduced follicular helper T (T_{FH}) cells, their ability to mount a humoral immune response to immunization or viral infection is impaired, similar to the ORAI1-deficient patients' inability to seroconvert after vaccination. The decreased numbers of Treg cells in ORAI1-deficient patients likely cause, together with chronic infections, the loss of naive T cells as well as the patients' autoimmunity and lymphadenopathy. Taken together, our findings suggest that SOCE is required for the development of agonist-selected iNKT and Tregs, whose lack likely contributes to the CID and autoimmunity observed in ORAI1-deficient patients.

A unifying feature of all patients with null mutations in *ORAI1* (and *STIM1*) is EDA. Anhidrosis was present in P1–P4 and confirmed by pilocarpin iontophoresis. It resulted in hyperthermia with severe attacks of facial blushing, tachycardia and tachypnea in P3 and P4. A skin biopsy of P1 confirmed the presence of eccrine sweat glands of normal morphology, which is consistent with similar findings in SOCE-deficient patients with ORAI1 p.R91W (P6) and STIM1 p.P165Q mutations [3, 50, 51]. We recently reported that sweat glands require

SOCE for the opening of the Ca^{2+}-activated chloride channel TMEM16A, and thus chloride secretion and sweat production [50]. Impaired sweat gland function as the cause of anhidrosis is different from patients with EDA-ID due to X-linked recessive mutations in *IKBKG* (NEMO, IKKγ) or autosomal dominant mutations in *NFKBIA* (Iκ-Bα) that suppress NF-κB signaling and are associated with absent eccrine sweat glands [36, 37, 52].

Another characteristic feature of EDA in P1–P4 (and other patients with *ORAI1* and *STIM1* mutations) is hypocalcified amelogenesis imperfecta (type III), a form of dental enamel hypoplasia that is due to defective calcification of the enamel matrix and use-dependent attrition of the enamel layer. ORAI1 is expressed in ameloblasts (cells that deposit dental enamel) where it likely mediates SOCE[53, 54]. An important role of SOCE in enamel formation (amelogenesis) was recently shown by us and others using $Stim1^{fl/fl}Stim2^{fl/fl}$ K14-Cre mice which have thin, mechanically weak and hypomineralized teeth with decreased Ca^{2+} content resulting in severe enamel attrition [55, 56]. Patients with EDA-ID due to *IKBKG* or *NFKBIA* (Iκ-Bα) mutations also have a tooth defect, which is characterized by hypodontia and conical teeth and thus morphologically easily distinguishable from the enamel defects in ORAI1-deficient patients [57–59]. EDA in P1–P4 furthermore manifested itself in thin and brittle hair, which in the case of P4 was prone to fall out. This hair phenotype is partially recapitulated in *Orai1*-deficient mice, which have progressive hair loss [60].

To date, the diagnosis EDA-ID is limited to patients with mutations in *IKBKG* (OMIM 300291) and *NFKBIA* genes (OMIM 164008), who present with hypotrichosis, hypodontia, hypohidrosis (EDA) and are prone to bacterial, viral and fungal infections (ID) [15]. Criteria for the diagnosis of EDA include sparse to absent hair, hypoplastic to absent sweat gland and hypodontia to adontia [59]. From a clinical perspective, patients with null mutations in *ORAI1* (or *STIM1*) fullfil 3 of these criteria: sparse hair, anhidrosis and amelogenesis imperfecta. With regard to immunodeficiency, mutations in *IKBKG* and *NFKBIA* increase susceptibility infections with mycobacteria, *Pneumocystis jiroveci,* C. albicans and, most frequently, pyogenic bacteria due to hypogammaglobulinemia and a failure to mount a specific antibody response to polysaccharide antigens [59]. ORAI1-deficient patients are susceptible to an overlapping spectrum of pathogens, but they are also prone to viral infections including CMV, EBV, RSV and Rotavirus. AIHA and autoimmune thrombocytopenia are common in patients with mutations in *ORAI1* and *STIM1* but not *IKBKG* and *NFKBIA;* instead patients with *IKBKG* mutation may develop inflammatory bowel disease (NEMO colitis) [59].

We here propose that mutations in *ORAI1* and *STIM1* constitute a new form of EDA-ID and are an important differential diagnosis of EDA-ID caused by mutations in *IKBKG* or *NFKBIA*.

Supplementary Material

Refer to Web version on PubMed Central for supplementary material.

Acknowledgments

Funding: This work was funded by NIH grants AI097302 (to S.F.), and AI065303 (to D.U.), postdoctoral fellowships KA 4514/1-1 (to S.K.) and VA 882/1-1 (to M.V.) by the German Research Foundation (Deutsche Forschungsgemeinschaft, DFG) and BMBF grant 01 EO 0803 by the German Federal Ministry of Education and Research (to S.E. and C.S.).

We thank Dr. H.J. McBride (Amgen, Thousand Oaks, CA) for providing the ORAI1 antibody used for FACS staining, Dr. A.F. Liang (Microscopy Core, NYU School of Medicine), Dr. A.M. Cuervo (Albert Einstein College of Medicine), Dr. R.T. Dirksen (University of Rochester) and the Feske lab for helpful discussions.

Abbreviations

Ca^{2+}	Calcium
$[Ca^{2+}]_i$	Intracellular calcium concentration
CID	Combined immunodeficiency
CRAC	Ca^{2+} release-activated Ca^{2+}
EDA-ID	Anhidrotic ectodermal dysplasia with immunodeficiency
HSCT	Hematopoietic stem cell transplantation
SOCE	Store-operated Ca^{2+} entry
STIM	Stromal interaction molecule

References

1. Roos J, DiGregorio PJ, Yeromin AV, Ohlsen K, Lioudyno M, Zhang S, et al. STIM1, an essential and conserved component of store-operated Ca2+ channel function. J Cell Biol. 2005; 169:435–45. [PubMed: 15866891]
2. Liou J, Kim ML, Heo WD, Jones JT, Myers JW, Ferrell JE Jr, et al. STIM is a Ca2+ sensor essential for Ca2+-store-depletion-triggered Ca2+ influx. Curr Biol. 2005; 15:1235–41. [PubMed: 16005298]
3. Feske S, Gwack Y, Prakriya M, Srikanth S, Puppel SH, Tanasa B, et al. A mutation in Orai1 causes immune deficiency by abrogating CRAC channel function. Nature. 2006; 441:179–85. [PubMed: 16582901]
4. Vig M, Peinelt C, Beck A, Koomoa DL, Rabah D, Koblan-Huberson M, et al. CRACM1 is a plasma membrane protein essential for store-operated Ca2+ entry. Science. 2006; 312:1220–3. [PubMed: 16645049]
5. Zhang SL, Yeromin AV, Zhang XH, Yu Y, Safrina O, Penna A, et al. Genome-wide RNAi screen of Ca(2+) influx identifies genes that regulate Ca(2+) release-activated Ca(2+) channel activity. Proc Natl Acad Sci U S A. 2006; 103:9357–62. [PubMed: 16751269]
6. Feske S, Skolnik EY, Prakriya M. Ion channels and transporters in lymphocyte function and immunity. Nat Rev Immunol. 2012; 12:532–47. [PubMed: 22699833]
7. Chou J, Badran YR, Yee CSK, Bainter W, Ohsumi TK, Al-Hammadi S, et al. A novel mutation in ORAI1 presenting with combined immunodeficiency and residual T cell function. J Allergy Clin Immunol. 2015 [Epub ahead of print].
8. Fuchs S, Rensing-Ehl A, Speckmann C, Bengsch B, Schmitt-Graeff A, Bondzio I, et al. Antiviral and regulatory T cell immunity in a patient with stromal interaction molecule 1 deficiency. Journal of immunology. 2012; 188:1523–33.
9. McCarl CA, Picard C, Khalil S, Kawasaki T, Rother J, Papolos A, et al. ORAI1 deficiency and lack of store-operated Ca2+ entry cause immunodeficiency, myopathy, and ectodermal dysplasia. J Allergy Clin Immunol. 2009; 124:1311–8. e7. [PubMed: 20004786]

10. Picard C, McCarl CA, Papolos A, Khalil S, Luthy K, Hivroz C, et al. STIM1 mutation associated with a syndrome of immunodeficiency and autoimmunity. N Engl J Med. 2009; 360:1971–80. [PubMed: 19420366]
11. Klemann C, Ammann S, Heizmann M, Fuchs S, Bode SF, Heeg M, et al. Hemophagocytic lymphohistiocytosis as presenting manifestation of profound combined immunodeficiency due to an ORAI1 mutation. J Allergy Clin Immunol. 2017
12. Picard C, Al-Herz W, Bousfiha A, Casanova JL, Chatila T, Conley ME, et al. Primary Immunodeficiency Diseases: an Update on the Classification from the International Union of Immunological Societies Expert Committee for Primary Immunodeficiency 2015. Journal of Clinical Immunology. 2015; 35:696–726. [PubMed: 26482257]
13. Lacruz RS, Feske S. Diseases caused by mutations in ORAI1 and STIM1. Ann N Y Acad Sci. 2015; 1356:45–79. [PubMed: 26469693]
14. Feske S. CRAC channelopathies. Pflugers Arch. 2010; 460:417–35. [PubMed: 20111871]
15. Picard C, Casanova JL, Puel A. Infectious Diseases in Patients with IRAK-4, MyD88, NEMO, or I kappa B alpha Deficiency. Clinical Microbiology Reviews. 2011; 24:490–7. [PubMed: 21734245]
16. Boisson B, Puel A, Picard C, Casanova JL. Human IkappaBalpha Gain of Function: a Severe and Syndromic Immunodeficiency. J Clin Immunol. 2017; 37:397–412. [PubMed: 28597146]
17. Maus M, Jairaman A, Stathopulos PB, Muik M, Fahrner M, Weidinger C, et al. Missense mutation in immunodeficient patients shows the multifunctional roles of coiled-coil domain 3 (CC3) in STIM1 activation. Proc Natl Acad Sci U S A. 2015; 112:6206–11. [PubMed: 25918394]
18. Feske S. Immunodeficiency due to defects in store-operated calcium entry. Ann N Y Acad Sci. 2011; 1238:74–90. [PubMed: 22129055]
19. Hou X, Pedi L, Diver MM, Long SB. Crystal structure of the calcium release-activated calcium channel Orai. Science. 2012; 338:1308–13. [PubMed: 23180775]
20. Yen M, Lokteva LA, Lewis RS. Functional Analysis of Orai1 Concatemers Supports a Hexameric Stoichiometry for the CRAC Channel. Biophysical Journal. 2016; 111:1897–907. [PubMed: 27806271]
21. Yamashita M, Yeung PSW, Ing CE, McNally BA, Pomes R, Prakriya M. STIM1 activates CRAC channels through rotation of the pore helix to open a hydrophobic gate. Nature Communications. 2017:8.
22. Prakriya M, Feske S, Gwack Y, Srikanth S, Rao A, Hogan PG. Orai1 is an essential pore subunit of the CRAC channel. Nature. 2006; 443:230–3. [PubMed: 16921383]
23. Lin FF, Elliott R, Colombero A, Gaida K, Kelley L, Moksa A, et al. Generation and Characterization of Fully Human Monoclonal Antibodies Against Human Orai1 for Autoimmune Disease. Journal of Pharmacology and Experimental Therapeutics. 2013; 345:225–38. [PubMed: 23475901]
24. Maul-Pavicic A, Chiang SC, Rensing-Ehl A, Jessen B, Fauriat C, Wood SM, et al. ORAI1-mediated calcium influx is required for human cytotoxic lymphocyte degranulation and target cell lysis. Proceedings of the National Academy of Sciences of the United States of America. 2011; 108:3324–9. [PubMed: 21300876]
25. Desvignes L, Weidinger C, Shaw P, Vaeth M, Ribierre T, Liu M, et al. STIM1 controls T cell-mediated immune regulation and inflammation in chronic infection. J Clin Invest. 2015
26. Elling R, Keller B, Weidinger C, Haffner M, Deshmukh SD, Zee I, et al. Preserved effector functions of human ORAI1- and STIM1-deficient neutrophils. J Allergy Clin Immunol. 2016; 137:1587–91. e7. [PubMed: 26670474]
27. Feske S, Muller JM, Graf D, Kroczek RA, Drager R, Niemeyer C, et al. Severe combined immunodeficiency due to defective binding of the nuclear factor of activated T cells in T lymphocytes of two male siblings. Eur J Immunol. 1996; 26:2119–26. [PubMed: 8814256]
28. Vaeth M, Eckstein M, Shaw PJ, Kozhaya L, Yang J, Berberich-Siebelt F, et al. Store-Operated Ca2+ Entry in Follicular T Cells Controls Humoral Immune Responses and Autoimmunity. Immunity. 2016; 44:1350–64. [PubMed: 27261277]
29. Yu N, Li XM, Song WY, Li DM, Yu DL, Zeng XF, et al. CD4(+)CD25(+)CD127(low/−) T Cells: A More Specific Treg Population in Human Peripheral Blood. Inflammation. 2012; 35:1773–80. [PubMed: 22752562]

30. Oh-hora M, Komatsu N, Pishyareh M, Feske S, Hori S, Taniguchi M, et al. Agonist-Selected T Cell Development Requires Strong T Cell Receptor Signaling and Store-Operated Calcium Entry. Immunity. 2013; 38:881–95. [PubMed: 23499491]

31. Crosby CM, Kronenberg M. Invariant natural killer T cells: front line fighters in the war against pathogenic microbes. Immunogenetics. 2016; 68:639–48. [PubMed: 27368411]

32. Vantourout P, Hayday A. Six-of-the-best: unique contributions of gammadelta T cells to immunology. Nat Rev Immunol. 2013; 13:88–100. [PubMed: 23348415]

33. Maus M, Cuk M, Patel B, Lian J, Ouimet M, Kaufmann U, et al. Store-Operated Ca2+ Entry Controls Induction of Lipolysis and the Transcriptional Reprogramming to Lipid Metabolism. Cell Metabolism. 2017; 25:698–712. [PubMed: 28132808]

34. Bohm J, Bulla M, Urquhart JE, Malfatti E, Williams SG, O'Sullivan J, et al. ORAI1 Mutations with Distinct Channel Gating Defects in Tubular Aggregate Myopathy. Hum Mutat. 2017; 38:426–38. [PubMed: 28058752]

35. Endo Y, Noguchi S, Hara Y, Hayashi YK, Motomura K, Miyatake S, et al. Dominant mutations in ORAI1 cause tubular aggregate myopathy with hypocalcemia via constitutive activation of store-operated Ca(2)(+) channels. Hum Mol Genet. 2015; 24:637–48. [PubMed: 25227914]

36. Doffinger R, Smahi A, Bessia C, Geissmann F, Feinberg J, Durandy A, et al. X-linked anhidrotic ectodermal dysplasia with immunodeficiency is caused by impaired NF-kappaB signaling. Nat Genet. 2001; 27:277–85. [PubMed: 11242109]

37. Jain A, Ma CA, Liu S, Brown M, Cohen J, Strober W. Specific missense mutations in NEMO result in hyper-IgM syndrome with hypohydrotic ectodermal dysplasia. Nat Immunol. 2001; 2:223–8. [PubMed: 11224521]

38. Zhang SL, Yeromin AV, Hu J, Amcheslavsky A, Zheng H, Cahalan MD. Mutations in Orai1 transmembrane segment 1 cause STIM1-independent activation of Orai1 channels at glycine 98 and channel closure at arginine 91. Proceedings of the National Academy of Sciences of the United States of America. 2011; 108:17838–43. [PubMed: 21987804]

39. McNally BA, Yamashita M, Engh A, Prakriya M. Structural determinants of ion permeation in CRAC channels. Proc Natl Acad Sci U S A. 2009; 106:22516–21. [PubMed: 20018736]

40. McNally BA, Somasundaram A, Yamashita M, Prakriya M. Gated regulation of CRAC channel ion selectivity by STIM1. Nature. 2012; 482:241–5. [PubMed: 22278058]

41. Kim KD, Srikanth S, Yee MK, Mock DC, Lawson GW, Gwack Y. ORAI1 deficiency impairs activated T cell death and enhances T cell survival. J Immunol. 2011; 187:3620–30. [PubMed: 21873530]

42. Mavilio D, Lombardo G, Benjamin J, Kim D, Follman D, Marcenaro E, et al. Characterization of CD56−/CD16+ natural killer (NK) cells: a highly dysfunctional NK subset expanded in HIV-infected viremic individuals. Proc Natl Acad Sci U S A. 2005; 102:2886–91. [PubMed: 15699323]

43. Bjorkstrom NK, Ljunggren HG, Sandberg JK. CD56 negative NK cells: origin, function, and role in chronic viral disease. Trends in Immunology. 2010; 31:401–6. [PubMed: 20829113]

44. Yokobori N, Schierloh P, Geffner L, Balboa L, Romero M, Musella R, et al. CD3 expression distinguishes two gammadeltaT cell receptor subsets with different phenotype and effector function in tuberculous pleurisy. Clin Exp Immunol. 2009; 157:385–94. [PubMed: 19664147]

45. Chowers Y, Holtmeier W, Harwood J, Morzycka-Wroblewska E, Kagnoff MF. The V delta 1 T cell receptor repertoire in human small intestine and colon. J Exp Med. 1994; 180:183–90. [PubMed: 8006582]

46. Das H, Sugita M, Brenner MB. Mechanisms of Vdelta1 gammadelta T cell activation by microbial components. J Immunol. 2004; 172:6578–86. [PubMed: 15153472]

47. Pitard V, Roumanes D, Lafarge X, Couzi L, Garrigue I, Lafon ME, et al. Long-term expansion of effector/memory Vdelta2-gammadelta T cells is a specific blood signature of CMV infection. Blood. 2008; 112:1317–24. [PubMed: 18539896]

48. Vaeth M, Yang J, Yamashita M, Zee I, Eckstein M, Knosp C, et al. ORAI2 modulates store-operated calcium entry and T cell-mediated immunity. Nat Commun. 2017; 8:14714. [PubMed: 28294127]

49. Oh-Hora M, Yamashita M, Hogan PG, Sharma S, Lamperti E, Chung W, et al. Dual functions for the endoplasmic reticulum calcium sensors STIM1 and STIM2 in T cell activation and tolerance. Nat Immunol. 2008; 9:432–43. [PubMed: 18327260]
50. Concepcion AR, Vaeth M, Wagner LE, Eckstein M, Hecht L, Yang J, et al. Store-operated Ca2+ entry regulates Ca2+-activated chloride channels and eccrine sweat gland function. Journal of Clinical Investigation. 2016; 126:4303–18. [PubMed: 27721237]
51. Schaballie H, Rodriguez R, Martin E, Moens L, Frans G, Lenoir C, et al. A novel hypomorphic mutation in STIM1 results in a late-onset immunodeficiency. J Allergy Clin Immunol. 2015
52. Zonana J, Elder ME, Schneider LC, Orlow SJ, Moss C, Golabi M, et al. A novel X-linked disorder of immune deficiency and hypohidrotic ectodermal dysplasia is allelic to incontinentia pigmenti and due to mutations in IKK-gamma (NEMO). Am J Hum Genet. 2000; 67:1555–62. [PubMed: 11047757]
53. Nurbaeva MK, Eckstein M, Concepcion AR, Smith CE, Srikanth S, Paine ML, et al. Dental enamel cells express functional SOCE channels. Sci Rep. 2015; 5:15803. [PubMed: 26515404]
54. Zheng L, Zinn V, Lefkelidou A, Taqi N, Chatzistavrou X, Balam T, et al. Orai1 expression pattern in tooth and craniofacial ectodermal tissues and potential functions during ameloblast differentiation. Dev Dyn. 2015; 244:1249–58. [PubMed: 26178077]
55. Eckstein M, Vaeth M, Fornai C, Vinu M, Bromage TG, Nurbaeva MK, et al. Store-operated Ca2+ entry controls ameloblast cell function and enamel development. JCI Insight. 2017; 2:e91166. [PubMed: 28352661]
56. Furukawa Y, Haruyama N, Nikaido M, Nakanishi M, Ryu N, Oh-Hora M, et al. Stim1 Regulates Enamel Mineralization and Ameloblast Modulation. J Dent Res. 2017 22034517719872.
57. Jorgensen SE, Bottger P, Kofod-Olsen E, Holm M, Mork N, Orntoft TF, et al. Ectodermal dysplasia with immunodeficiency caused by a branch-point mutation in IKBKG/NEMO. J Allergy Clin Immunol. 2016; 138:1706–9. e4. [PubMed: 27477329]
58. Courtois G, Smahi A, Reichenbach J, Doffinger R, Cancrini C, Bonnet M, et al. A hypermorphic IkappaBalpha mutation is associated with autosomal dominant anhidrotic ectodermal dysplasia and T cell immunodeficiency. J Clin Invest. 2003; 112:1108–15. [PubMed: 14523047]
59. Kawai T, Nishikomori R, Heike T. Diagnosis and treatment in anhidrotic ectodermal dysplasia with immunodeficiency. Allergol Int. 2012; 61:207–17. [PubMed: 22635013]
60. Gwack Y, Srikanth S, Oh-Hora M, Hogan PG, Lamperti ED, Yamashita M, et al. Hair loss and defective T- and B-cell function in mice lacking ORAI1. Mol Cell Biol. 2008; 28:5209–22. [PubMed: 18591248]

Clinical implications

Mutations in *ORAI1* (or *STIM1*) that abolish SOCE cause a new form of EDA with immunodeficiency (EDA-ID) that has to be differentiated from EDA-ID due to defects in NF-κB signaling.

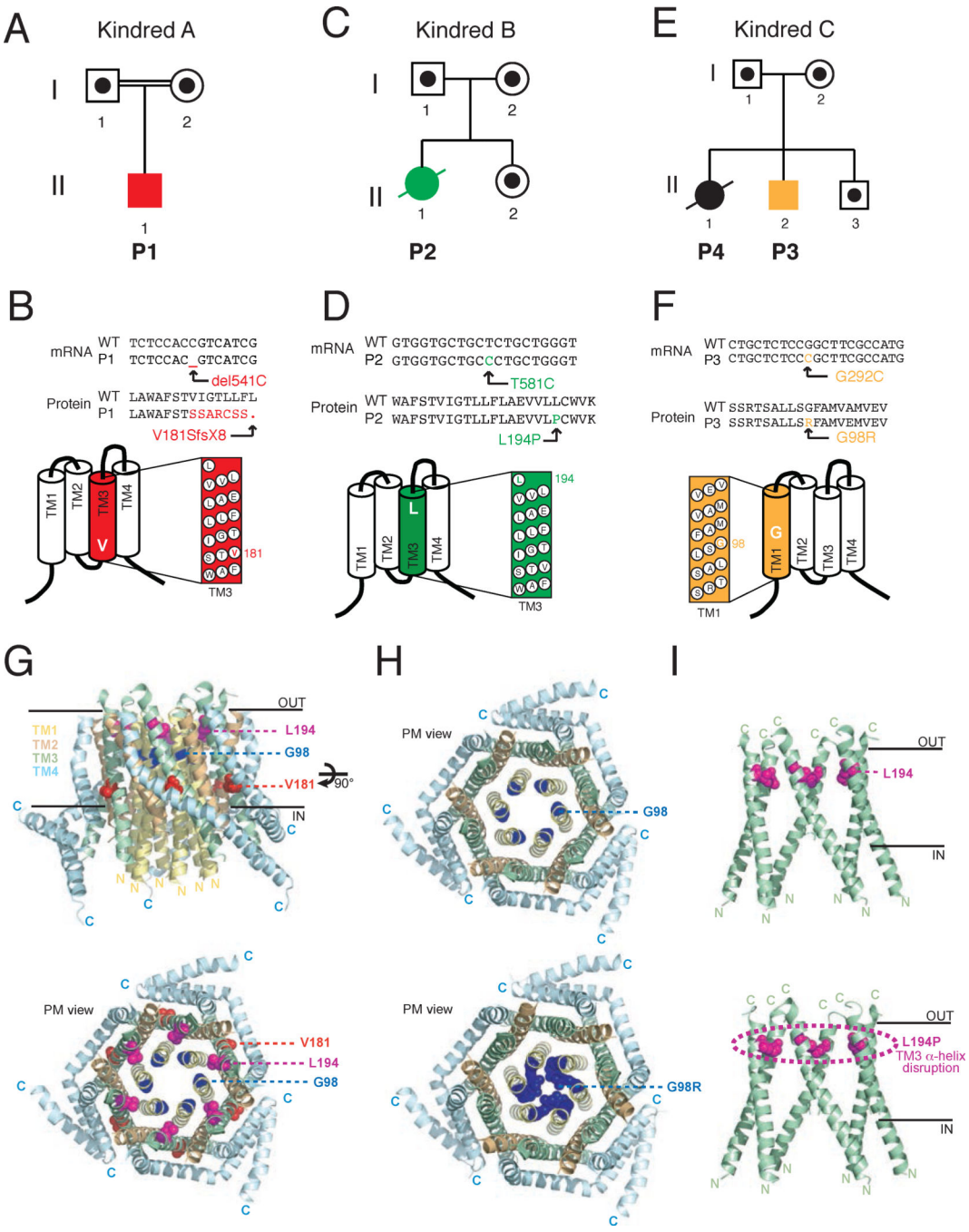

Figure 1. Three novel autosomal recessive *ORAI1* mutations associated with CRAC channelopathy

A–F, Pedigrees (**A,C,E**) and mRNA/protein sequences of *ORAI1* mutations (**B,D,F**) identified in three unrelated kindreds. **A,B,** Patient 1 (P1, A-II-1) of kindred A is homozygous for a single nucleotide deletion (c.del541C) in exon 2 of *ORAI1* that results in a frameshift and premature stop codon at V181SfsX8 in the third transmembrane domain (TM3) of ORAI1 protein. **C,D,** P2 (B-II-1) is homozygous for a single nucleotide transition (c.T581C) in exon 2 of *ORAI1* that results in a single amino acid substitution in TM3

(p.L194P). **E,F,** P3 (C-II-2) and his sister P4 (C-II-1) are homozygous for a single nucleotide transversion (c.G292C) in exon 1 of *ORAI1* that results in a single amino acid substitution in TM1 (p.G98R). Filled symbols in A, C, E represent patients; dots in empty symbols represent confirmed heterozygous carriers; double lines indicate consanguinity. **G**, Homology model of the hexameric human ORAI1 protein structure modeled on the *D. melanogaster* Orai crystal structure [19]. Tertiary structure of the ORAI1 hexamer from the side (top) and the extracellular side of the plasma membrane (PM) revealing the channel pore (bottom). The inner (IN) and outer (OUT) leaflets of the PM are indicated; TM domains are color coded (TM1: yellow; TM2 orange; TM3: green; TM4 blue). Amino acid residues mutated in P1–P4 are shown in color (V181: red; L194: magenta; G98: blue). **H–I**, Structure models of wildtype (top) and mutant (bottom) ORAI1 (H: L194P; I: G98R). The models orient the mutant side chains in positions homologous to the wildtype residues and do not show an experimentally determined structure of mutant proteins.

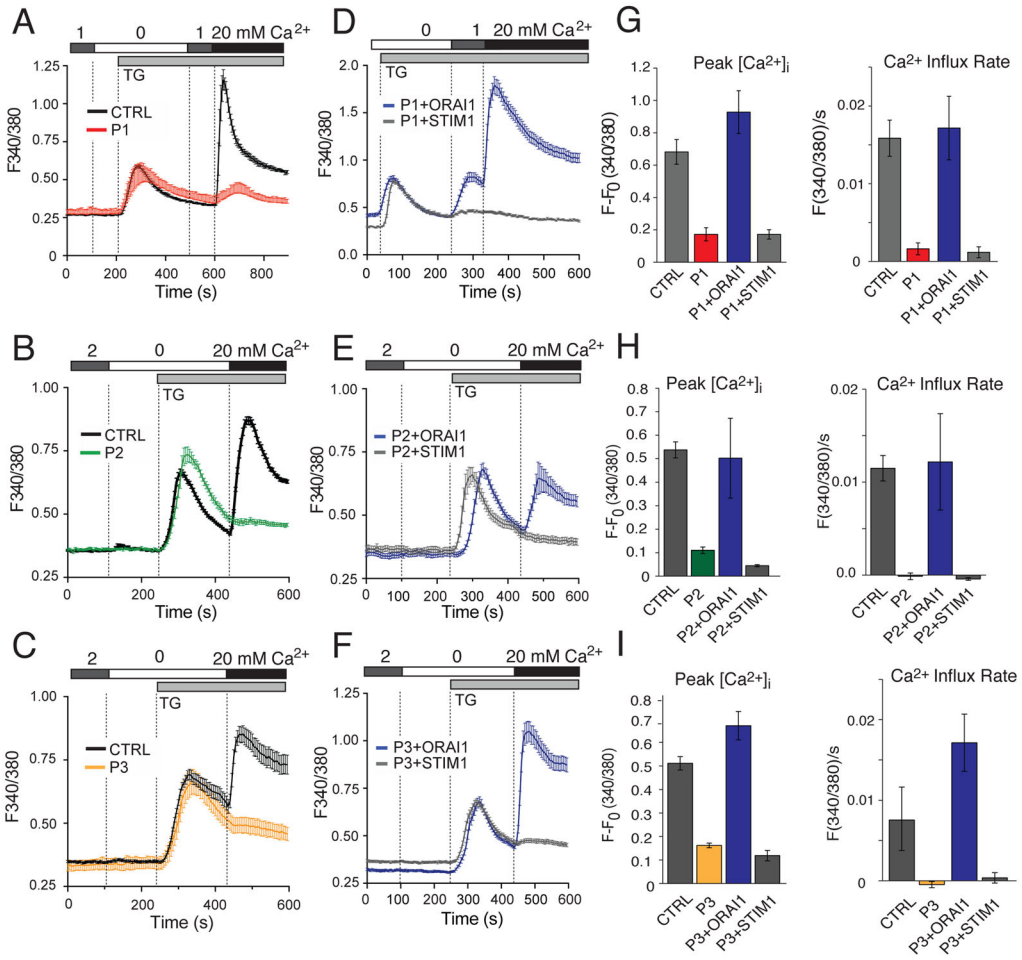

Figure 2. *ORAI1* mutations abolish SOCE

A–C, SOCE measurements in fibroblasts of P1, P2, P3 and a HD control (CTRL). Cells were loaded with Fura-2 and stimulated with thapsigargin (TG) in the absence of extracellular Ca^{2+} followed by readdition of 20 mM Ca^{2+}. Traces show intracellular Ca^{2+} levels (F340/380) recorded by time-lapse microscopy and represent the average ± SEM of > 64 cells from one representative experiment. **D–F**, Fibroblasts from P1, P2 and P3 were retrovirally transduced with bicistronic vectors encoding wildtype ORAI1 (IRES-GFP) or STIM1 (IRES-GFP). Intracellular Ca^{2+} levels in GFP^{+} fibroblasts were measured as described in A–C. Shown are Ca^{2+} traces from one representative experiment; > 30 cells were analyzed. **G–I**, Bar graphs show the mean ± SEM of peak intracellular Ca^{2+} levels after TG stimulation and readdition of 20 mM Ca^{2+}(left) and the Ca^{2+} influx rate in the first 20 s after readdition of Ca^{2+}(right). Ca^{2+} traces in A–F and bar graphs in G–I are representative of two (P2, P3) and three (P1) independent experiments.

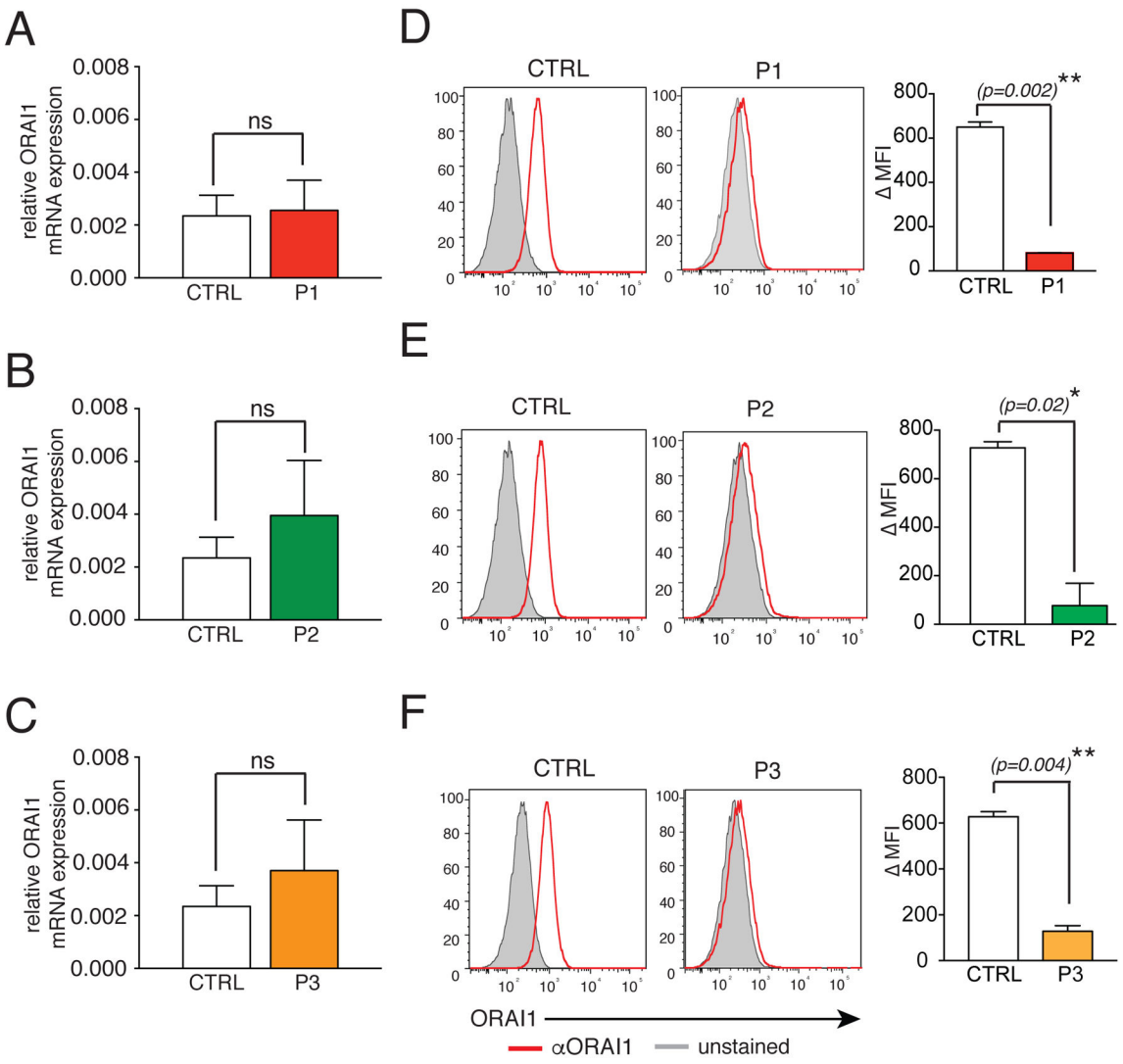

Figure 3. *ORAI1* mutations abolish protein expression

A–C, Bar graphs show the mean ± SEM of ORAI1 mRNA isolated from fibroblasts of P1 (A), P2 (B) and P3 (C) compared to HD control fibroblasts (CTRL) and measured by qPCR. **D–F,** Flow cytometric analysis of ORAI1 (red) at the surface of fibroblasts from P1 (D), P2 (E), P3 (F) and HD control fibroblasts (CTRL) using an antibody against the second extracellular domain of ORAI1. Unstained fibroblasts were used as control (gray). Bar graphs show the average of ΔMFIs (calculated as $MFI_{ORAI1} - MFI_{unstained\ control}$) ± SEM. Data in A–C and D–F represent 2 independent experiments for each patient. Statistical significance was calculated using unpaired Student's t test, $p<0.05$*, $p<0.01$**.

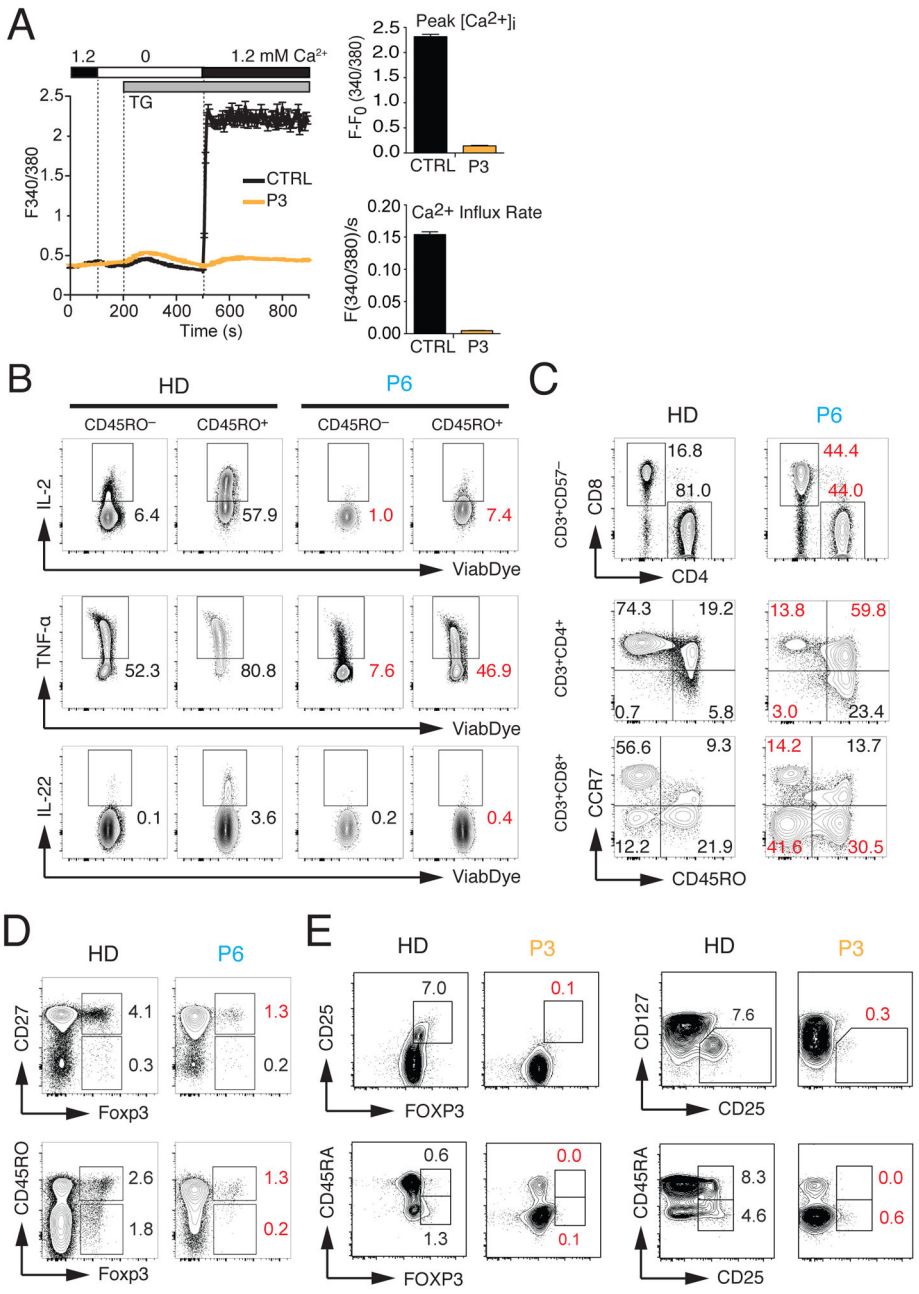

Figure 4. Impaired T cell function and reduced numbers of regulatory T cells in ORAI1 deficient patients

A, Measurements of SOCE in T cells from P3 and a healthy control (CTRL) by time-lapse microscopy. Cells were stimulated with thapsigargin (TG) followed by readdition of 1.2 mM extracellular Ca^{2+}. Traces show intracellular Ca^{2+} levels (F340/380) of > 60 cells (average ± SEM). Bar graphs represent the mean ± SEM of the SOCE peak in 1.2 mM Ca^{2+} (top) and the Ca^{2+} influx rate in the first 20 s after readdition of Ca^{2+}(bottom). Data are representative for three experiments. **B,** Cytokine production by PBMC from P6 (ORAI1 p.R91W) [3] isolated at 20 years of age and an adult HD control. PBMC were stimulated with PMA (40 ng/ml) and ionomycin (500 ng/ml) for 4 hours, and analyzed by intracellular cytokine

staining and flow cytometry. **C**–**D**, Flow cytometry analysis of PBMC from the 20-year-old P6 and a representative HD control for naïve, central memory and effector memory $CD4^+$ and $CD8^+$ T cells (**C**) and $Foxp3^+$ Treg cells (**D**). **E,** Flow cytometry analysis of PBMC from P3 (ORAI1 p.G98R) and a HD control for $Foxp3^+$ Treg cells. Contour plots are gated on $CD4^+$ cells. Numbers in red in panels B–E indicate marked differences in T cell subsets in P6 compared to HD controls.

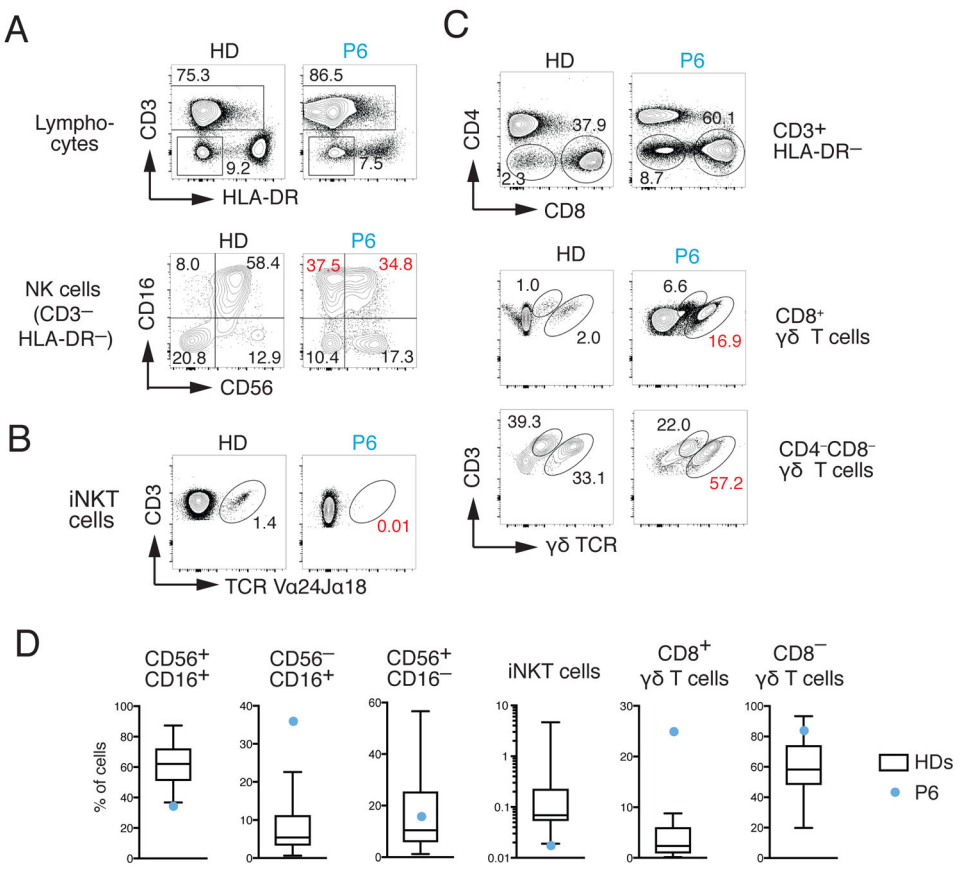

Figure 5. Lack of iNKT cells and perturbed NK and γδ T cell populations in ORAI1 deficient patient

A–**C**, Flow cytometry analysis of PBMCs from the 20-year-old P6 and a representative HD control for NK cells (A), iNKT cells (B) and γδ T cells (C). **A**, For the detection of NK cells, $CD3^-$ $HLA\text{-}DR^-$ lymphocytes were stained with antibodies against CD16 and CD56. **B**, For the detection of iNKT cells, lymphocytes were stained with antibodies against CD3 and the Vα24Jα18 TCR. **C,** For the detection of $CD4^-CD8^+$ and $CD4^-CD8^-$ γδ T cells, lymphocytes were stained with antibodies against CD3 and the γδ TCR. Numbers in red in panels A–C indicate marked differences in T cell subsets in P6 compared to HD controls. **D**, Frequencies of $CD16^+CD56^+$, $CD16^-CD56^+$ and $CD16^+CD56^-$ NK cells, $CD3^+$ $Vα24Jα18^+$ iNKT cells and $CD4^-CD8^+$ or $CD4^-CD8^-$ γδ T cells in PBMC of P6 (blue circles) from panels A–C compared to 23 unrelated HD controls (aged 22–65 years). Whisker plots show the median, 25–75 percentiles and minimum and maximum values of the distribution of HDs.

Table 1

Summary of clinical and laboratory findings in P1–P4.

Patient	**P1 (A-II-1)**	**P2 (B-II-1)**	**P3 (C-II-2)**	**P4 (C-II-1)**	**P5***	**P6***
Inheritance	AR	AR	AR	AR	AR	AR
Type of mutation	1nt deletion (del541C)	Missense (T581C)	Missense (G292C)	Missense (G292C)	Missense (C271T)	Missense (C271T)
***ORAI1* mutation**	p.V181SfsX8	p.L194P	p.G98R	p.G98R	p.R91W	p.R91W
ORAI1 expression	mRNA: normal Protein: abolished	mRNA: normal Protein: abolished	mRNA: normal Protein: abolished	mRNA: n. t. Protein: n.t.	mRNA: normal Protein: normal	mRNA: normal Protein: normal
SOCE	abolished	abolished	Abolished	n.t.	abolished	abolished
SOCE defect observed in	Fibroblasts	Fibroblasts	Fibroblasts and T cells	n.t.	Fibroblasts and T cells	Fibroblasts, T cells, B cells
Infections	Rotavirus enteritis, Pneumocystis jirovecii pneumonia	Klebsiella pneumoniae and Candida albicans sepsis, Staphylococcus aureus pneumonia, CMV pneumonitis, Enterobacter cloacae sepsis, Norovirus and Salmonella enteritidis gastroenteritis, bacterial Meningitis	RSV and Rotavirus, Therapy-resistant CMV pneumonias, Stenotrophomonas maltophilia, Extended- spectrum β-lactamase-producing Klebsiella pneumoniae, Candida albicans, Aspergillus fumigatus, BCGitis after vaccination	Pseudomonas aeruginosa, Staphylococcus aureus, Klebsiella pneumoniae, Streptococcus pneumoniae, Aspergillus fumigatus, Candida albicans, Respiratory syncytial virus, Adenovirus, Influenza, Parainfluenza, disseminated cytomegalovirus sepsis with encephalitis, pneumonitis, colitis, chorioretinitis and adrenalitis, BCGitis after vaccination, Acinetobacter baumanii, Enterococcus faecalis, Rotavirus, Adenovirus	BCGitis, Meningitis, Rotavirus enteritis, Interstitial pneumonia, GI sepsis	Rotavirus enteritis
Autoimmunity	n.r.	Anemia, Thrombocytopenia	Coombs positive autoimmune hemolytic anemia (AIHA), anti-cardiolipin Abs, ANA and ANCA	Coombs positive AIHA, Antiphospholipid syndrome (anti-cardiolipin and anti-β2-glycoprotein 1 antibodies), autoimmune neutropenia and thrombocytopenia	n.r.	ANA^+
Lymphocytes	naïve $CD45RA^+$ T cells ↓	Normal	$CD4^+$ T cells ↑, $CD8^+$ T cells ↓, naïve $CD45RA^+$ T cells ↓, $CD4^+CD25^+Foxp3^+$ regulatory T cells ↓	$CD4^+$ T cells ↑ $CD8^+$ T cells ↓	$CD3^+HLA\text{-}DR^+$ ↑, $CD4^+CD29^+$ ↑	$CD3^+HLA\text{-}DR^+$ ↑, $CD4^+CD29^+$ ↑ $CD4^+CD25^+Foxp3^+$ regulatory T cells ↓, NK and iNKT cells ↓, d γδT cells ↑
Lymphocyte function	T cell proliferation ↓↓	IFN-γ production ↓	T cell proliferation ↓	IFN-γ and IL-4 production ↓	T cell proliferation ↓ Cytokine production ↓	T cell proliferation ↓ Cytokine production ↓
Antibodies	oligoclonal IgA ↑, IgM ↑, λ chains ↑, no seroconversion	Hyper/dysgammaglobulinemia (IgA, IgG, IgM ↑)	IgE ↑	IgA/IgG inversion, IgE ↑, IgM/IgG/IgA against red blood cells and platelets	Normal to ↑ Ig levels No specific Ab response	Normal to ↑ Ig levels No specific Ab response
Myopathy	Congenital muscular hypotonia with type 2 muscle fiber atrophy, esotropia	Congenital muscular hypotonia	Congenital muscular hypotonia, partial iris hypoplasia	Congenital muscular hypotonia	Congenital muscular hypotonia, mydriasis	Congenital muscular hypotonia
Anhidrotic Ectodermal Dysplasia (EDA)	Anhidrosis, dental enamel hypoplasia, mild hypotrichosis	Anhidrosis, sparse/thin/brittle hair Teeth: n.r.**	Anhidrosis, dry and exfoliate skin, sparse/thin/brittle hair, Hypocalcified amelogenesis imperfecta (type III)	Anhidrosis, dry and exfoliate skin, sparse/thin/ brittle hair, dental enamel hypoplasia	n.r.**	Anhidrosis, Hypocalcified amelogenesis imperfecta (type III)

Patient	P1 (A-II-1)	P2 (B-II-1)	P3 (C-II-2)	P4 (C-II-1)	P5*	P6*
Other complications	Pathological fractures after trivial traumata, mineral bone density ↓	Hepatosplenomegaly, lymphadenopathy	Hepatosplenomegaly, CNS: atrophy of deep white matter around peritrigonal area of the brain	Hepatosplenomegaly, lymphadenopathy	small thymus	bronchiectasis
Outcome	HSCT at 13 mo.	deceased at 7.5 mo.	HSCT at 7 mo; post-HSCT complications: CMV infections, AIHA, skin GVHD, hepatic veno-occlusive disease, BCGitis	deceased at 2.5 yrs	deceased at 11 mo.	1st HSCT at 4 mo.; loss of donor chimerism and CMV infection at 19 yrs; isolation of PBMC before 2nd HSCT at 20 yrs

Abbreviations: AR, autosomal recessive; Ig, Immunoglobulin; HSCT, Hematopoietic stem cell transplantation; mo, months; n.r., not reported; n.t., not tested; yrs, years

*for detailed case report of P5 and P6 see Feske et al. (1996) and Feske et al. (2000)

**patient died before complete dentition